Broadband inelastic light scattering study on relaxor ferroelectric Pb(In1/2Nb1/2)-Pb(Mg1/3Nb2/3)O3-PbTiO3 single crystals

Tae Hyun Kim, Seiji Kojima, and Jae-Hyeon Ko

Citation: Journal of Applied Physics **115**, 234103 (2014); doi: 10.1063/1.4878855
View online: http://dx.doi.org/10.1063/1.4878855
View Table of Contents: http://scitation.aip.org/content/aip/journal/jap/115/23?ver=pdfcov
Published by the AIP Publishing

Broadband inelastic light scattering study on relaxor ferroelectric $Pb(In_{1/2}Nb_{1/2})$-$Pb(Mg_{1/3}Nb_{2/3})O_3$-$PbTiO_3$ single crystals

Tae Hyun Kim,[1] Seiji Kojima,[1,a)] and Jae-Hyeon Ko[2,b)]
[1]*Graduate School of Pure and Applied Physics, University of Tsukuba, Tsukuba, Ibaraki 305-8573, Japan*
[2]*Department of Physics, Hallym University, 39 Hallymdaehakgil 39, Chuncheon, Gangwondo 200-702, South Korea*

(Received 3 April 2014; accepted 5 May 2014; published online 16 June 2014)

The broadband inelastic light scattering spectra of ternary $Pb(In_{1/2}Nb_{1/2})$-$Pb(Mg_{1/3}Nb_{2/3})O_3$-$PbTiO_3$ single crystals were investigated as a function of temperature and crystal orientation by combining Raman and Brillouin spectroscopies. The angular dependence of the strong Raman peak located at $\sim 50\,cm^{-1}$ was investigated at 300 °C. The intensity variation of this mode with rotation angle was compatible with the F_{2g} mode of $Fm\bar{3}m$ symmetry, suggesting that this mode arises from the 1:1 chemical order at the B-site in this perovskite structure. The temperature evolution of the polar nanoregions was associated with the growth of two central peaks and the change in the intensity of some Raman peaks, which were known to be sensitive to the rhombohedral symmetry. Both relaxation processes exhibited partial slowing-down behaviors with a common critical temperature of ~160 °C. Poling the crystal along the [001] direction induced abrupt changes in some of the Raman bands at the rhombohedral–tetragonal phase transition. On the other hand, the diffuse tetragonal–cubic phase transition was not affected by the poling process. This high-temperature phase transformation seems to be smeared out by the inherent disorder and strong random fields enhanced by the addition of $Pb(In_{1/2}Nb_{1/2})$ into $Pb(Mg_{1/3}Nb_{2/3})O_3$-$PbTiO_3$. © *2014 AIP Publishing LLC*. [http://dx.doi.org/10.1063/1.4878855]

I. INTRODUCTION

Binary relaxor-based ferroelectric single crystals, such as $(1-x)Pb(Mg_{1/3}Nb_{2/3})O_3$-$xPbTiO_3$ (PMN-xPT) and $(1-x)Pb(Zn_{1/3}Nb_{2/3})O_3$-$xPbTiO_3$ (PZN-xPT), near the morphotropic phase boundary (MPB) have attracted high attention because of their superior piezoelectric ($d_{33} > 1500\,pC/N$) and electromechanical properties ($k_{33} > 0.9$).[1] These complex perovskite solid solutions have already been adopted in various piezoelectric applications as actuators, transducers, etc., but they suffer from some shortcomings, e.g., low coercive fields and low phase transition temperatures. These properties limit the device application range in both temperature and electric-field windows. Recently, ternary relaxor ferroelectric single crystals of $Pb(In_{1/2}Nb_{1/2})$-$Pb(Mg_{1/3}Nb_{2/3})O_3$-$PbTiO_3$ (PIN– PMN–PT) with compositions near MPB have been explored extensively due to their higher coercive fields, excellent piezoelectric performances, and higher phase transition temperatures than the binary systems.[2–15] Besides the superior characteristics of PIN-PMN-PT from the viewpoint of applications, it exhibits complex phase transition behaviors owing to the enhanced frustration, which needs more investigation from the fundamental point of view.[16–18] In particular, the effect of the antiferroelectric interaction arising from the addition of PIN with B-site ordering on the diffuse phase transition remains unsettled and should be revealed in more detail.

In spite of recent thorough studies on ternary PIN-PMN-PT single crystals, most studies have focused on macroscopic properties of this system, such as dielectric and piezoelectric characteristics.[2–18] In order to get more insights into the nature of phase transition behaviors, some experimental methods with different length and time scales other than the macroscopic measurements are necessary. In this sense, broadband inelastic light scattering spectroscopy can be an appropriate approach, because it is very sensitive to structural transformations occurring on a very short length and time scales and thus to local symmetry changes. In particular, it has been a powerful tool in the investigation of structural characteristics of relaxors on the nanometer scale, such as polar nanoregions (PNR) and chemically ordered regions (COR) in relaxor ferroelectrics.[19–26] In addition, low-frequency (low-wavenumber) spectral range is very important because soft optic phonon mode and/or central peak (CP) can be probed and investigated in relation to the nature of phase transition behaviors and relaxation dynamics.[27–29]

The motivation of the present study is to carry out systematic investigation of PIN-PMN-PT single crystals by using a high-resolution Raman spectroscopy with the high stray light rejection, including polarization effect, temperature, and angular dependences of vibrational spectra. In addition, we examined the relaxational dynamics of PNR by combining the quasi-elastic spectra measured by both Brillouin and Raman spectroscopy. This unified approach[28] is very promising for the accurate analysis of relaxational dynamics because many previous studies on the central peak behaviors have been handled separately in either the Brillouin or Raman frequency window.

a)Electronic mail: kojima@bk.tsukuba.ac.jp
b)Electronic mail: hwangko@hallym.ac.kr

II. EXPERIMENT

A. Experimental details

The ternary 0.26PIN-0.46PMN-0.28PT single crystals were grown using the modified Bridgman method (TRS Technologies Inc). Samples were cut into (001)-oriented platelets, which were polished to optical quality. The largest (001) surfaces of some samples were vacuum-sputtered by gold to apply an external electric field. In this case, the crystal was poled at 15 kV/cm immersed in silicon oil at room temperature to prevent arcing.

The Brillouin and Raman spectra for both [001]-poled and unpoled PIN-PMN-PT single crystals were collected in the macroconfiguration (BX-60, Olympus) and backscattering geometry (spot diameter $\sim 5\,\mu$m). The sample temperature was controlled by using a cryostat developed for a microscope (THMS600, Linkam) with a stability of $\pm 0.1\,^{\circ}$C. The Brillouin spectra were obtained by using a 6-pass tandem Fabry-Perot interferometer (TFP-1, JRS Co.) with a free spectral range of 300 GHz for CP. A diode-pumped solid-state (DPSS) laser (Compass 315M-100, Coherent) with single frequency operation at 532 nm was used for Brillouin scattering. The Raman scattering experiment was carried by using a triple-grating Raman spectrometer of additive dispersion (T64000, Jobin Yvon) combined with a photomultiplier tube (R464, Hamamatsu). The excitation source for Raman scattering was also a DPSS laser (Ventus, Laser Quantum) with a wavelength of 532 nm. All spectra were recorded with a spectral range from -100 to 950 cm^{-1} and spectral resolution of about 1.5 cm^{-1}. To protect the photomultiplier from the strong Rayleigh scattering, the spectral region from -10 to $+10$ cm^{-1} was excluded from the acquisition. In order to investigate angular dependence of Raman spectra at 300 °C, we measured polarized (VV) and depolarized (VH) Raman spectra at the $z(x,x)\bar{z}$ and $z(x,y)\bar{z}$ scattering geometries, respectively. These coordinates are expressed with respect to the pseudo-cubic crystal axes. For this measurement, a modified microscope was used, where a 1/2 λ wave-plate was inserted to control the polarization directions of the incident laser beam and the scattered light.[25]

B. Analysis

The polarized Raman spectra of unpoled PIN-PMN-PT measured at 30 °C are shown in Fig. 1 along with the reduced intensity by considering the Bose-Einstein population factor. As can be seen from these spectra, all phonon modes are broad and seem to partly overlap. In order to derive the phonon frequencies, line widths, and line-shape parameters of CP from the measured spectra, we directly decomposed the measured spectra using a multiple-peak fitting procedure. The Bose-Einstein factor F of Eq. (1) was considered in the fitting process,[19–21]

$$F(\omega,T)=\begin{cases} n(\omega)+1, & \text{for Stokes part} \\ n(\omega), & \text{for anti}-\text{Stokes part}, \end{cases} \quad (1)$$

where $n(\omega)=1/\{\exp(\frac{\hbar\omega}{kT})-1\}$, $\hbar$ the Planck constant, ω the angular frequency, k the Boltzmann constant, and T the temperature. The best-fitted result could be achieved with the assumption of a Lorentzian-type CP by the high-temperature approximation and the spectral response function of a damped harmonic oscillator for phonon modes, the latter being modified by the Bose-Einstein factor as follows:

$$I(\omega)=\frac{A}{\pi}\frac{\Delta\omega}{4\omega^2+\Delta\omega^2}+F(\omega,T)\sum_i \frac{2A_i\Gamma_i\omega_i^2\omega}{(\omega^2-\omega_i^2)^2+4\omega^2\Gamma_i^2}. \quad (2)$$

In Eq. (2), A and $\Delta\omega$ are the proportional constant and the width of CP, respectively. A_i, ω_i, and Γ_i are the amplitude, peak position, and damping constant, respectively, of the ith Raman mode. $\Delta\omega$ of CP is usually considered to be related to $1/\pi\tau$, where τ denotes a relaxation time of the relevant relaxation process responsible for the formation of CP.[27–29]

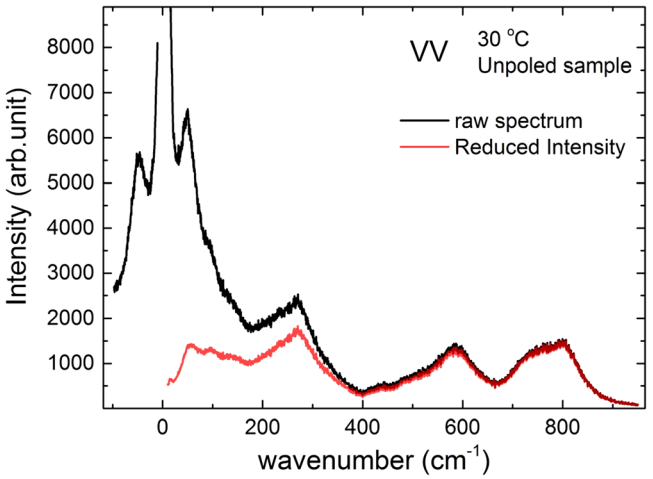

FIG. 1. Polarized Raman spectra from raw data (black line) and the one with reduced intensity corrected by the Bose-Einstein population factor (red line).

III. RESULTS AND DISCUSSION

A. Angular dependence of Raman spectra in unpoled PIN-PMN-PT

The first-order Raman spectrum in the cubic phase of $Pm\bar{3}m$ symmetry is forbidden in principle. Previous Raman studies on relaxors have shown first-order Raman peaks in the paraelectric phase of typical relaxors such as PMN, and the existence of COR and/or PNR was considered as possible origins.[19–26] The COR with a $Fm\bar{3}m$ symmetry originates from the chemical 1:1 order in the B-site of the perovskite structure. Recently, the angular dependence of the strong low-frequency mode of PMN near 45 cm^{-1} was measured and analyzed, which clearly showed that this peak corresponds to the F_{2g} mode of $Fm\bar{3}m$ symmetry.[25] However, there has been no experimental study reporting the existence of COR in the ternary PIN-PMN-PT system.

Figs. 2(a) and 2(b) show the angular dependence of Raman spectra in unpoled 0.26PIN-0.46PMN-0.28PT measured at 300 °C and observed at the VV and VH configurations, respectively. The Raman spectrum changes periodically with rotation angle. In particular, the intense peak at around 50 cm^{-1}, indicated by solid red circles,

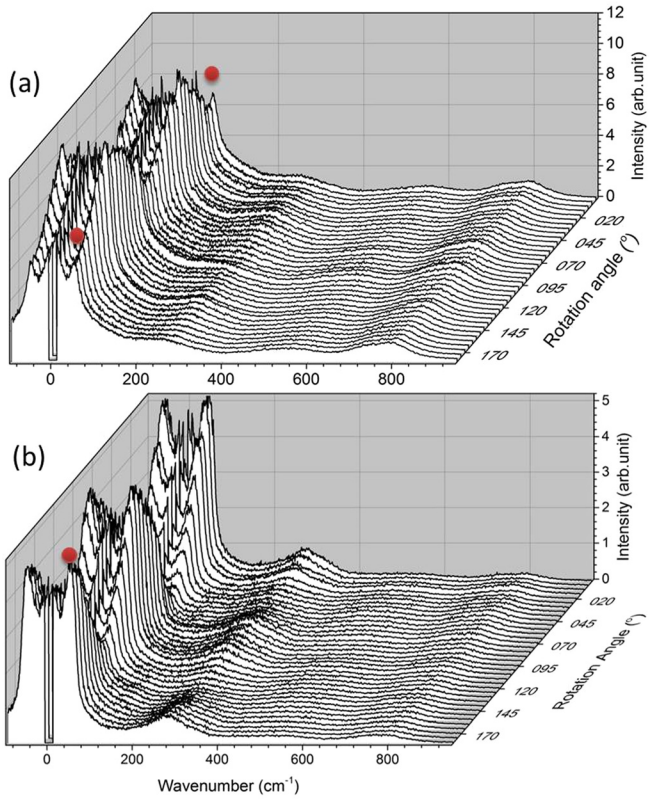

FIG. 2. Angular dependences of the Raman spectra in unpoled PIN-PMN-PT. (a) and (b) present the spectra observed at the VV and VH configurations, respectively. The red solid circles denote the strong line located near 50 cm^{-1}.

changes in intensity markedly. However, the angular variation of the intensities of other peaks is smaller compared to the case of PMN crystal.[25] According to the group theoretical analysis, there are four Raman active modes, $2\,F_{2g} + E_g + A_{1g}$, in the $Fm\bar{3}m$ symmetry. The angular dependence of the Raman intensity was suggested to be proportional to $\vec{R}^{-1} \cdot (A_{1g}$ or E_g or $F_{2g}) \cdot \vec{R}$, where $\vec{R}$ is the rotation matrix.[25] In case of PMN, the observed intensity of the band located near 45 cm^{-1} showed the angular variation compatible with the calculated results as described above. This showed that this component is due to the chemically ordered regions having a $Fm\bar{3}m$ symmetry.[25]

Figure 3(a) shows the extended view of the Raman spectrum of a 0.26PIN-0.46PMN-0.28PT single crystal in the low-frequency region. The periodic change in the Raman intensity of the low-frequency mode is clearly seen. The observed intensity variation for the low-frequency component at ~50 cm^{-1} is shown in Fig. 3(b). The oscillating behavior could be nicely fitted by using the variation of $\sin 2\theta$ according to $\vec{R}^{-1} \cdot F_{2g} \cdot \vec{R}$, similar to the case of PMN.[25] This result clearly shows that the strong peak near 50 cm^{-1} of PIN-PMN-PT is the F_{2g} mode of $Fm\bar{3}m$ symmetry. This also indicates that the observed angular dependence of this mode is not consistent with the $R3m$ symmetry. In spite of the recent extensive study on PIN-PMN-PT single crystals, the atomistic arrangement of cations has not been investigated in detail. The present result clearly suggests that there are chemically ordered regions in 0.26PIN-0.46PMN-0.28PT, where 1:1 ordered B-site cations

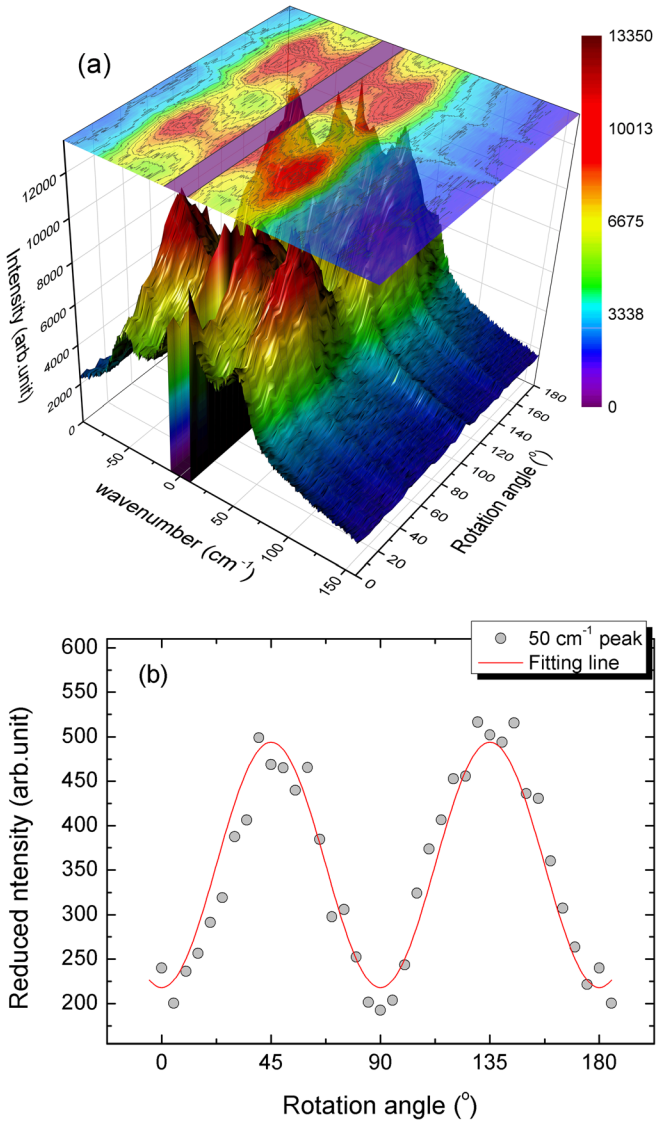

FIG. 3. (a) A contour map of the polarized (VV) Raman spectra observed from an unpoled PIN-PMN-PT crystal versus the rotation angle and the wavenumber (−100–150 cm^{-1}). (b) Angular dependence of intensity of the Raman peak located at ~50 cm^{-1} (circles) along with the calculated results based on Raman tensor analysis (solid line). See the text for more details.

exhibit $Fm\bar{3}m$ symmetry. In case of PMN-xPT, there is no COR at high PT concentration with $x > 0.21$.[23] In case of 0.26PIN-0.46PMN-0.28PT, COR seems to be persistent in spite of the high PT concentration of 28%, which may be attributed to the more complex disordered matrix formed by including the antiferroelectric PIN composition. It is well known that the complete 1:1 cation order at the B-site of PIN induces long-range antiferroelectric order at low temperatures.[30]

B. Temperature dependence of Raman spectra

The deconvolution of Raman spectra of an unpoled 0.26PIN-0.46PMN-0.28PT crystal is presented in Fig. 4. At 30 °C, a polarized spectrum is decomposed into 9 lines. In case of the unpoled sample, there are no appreciable changes in the peak frequencies of Raman bands depending on temperature in the measured temperature range. The depolarized

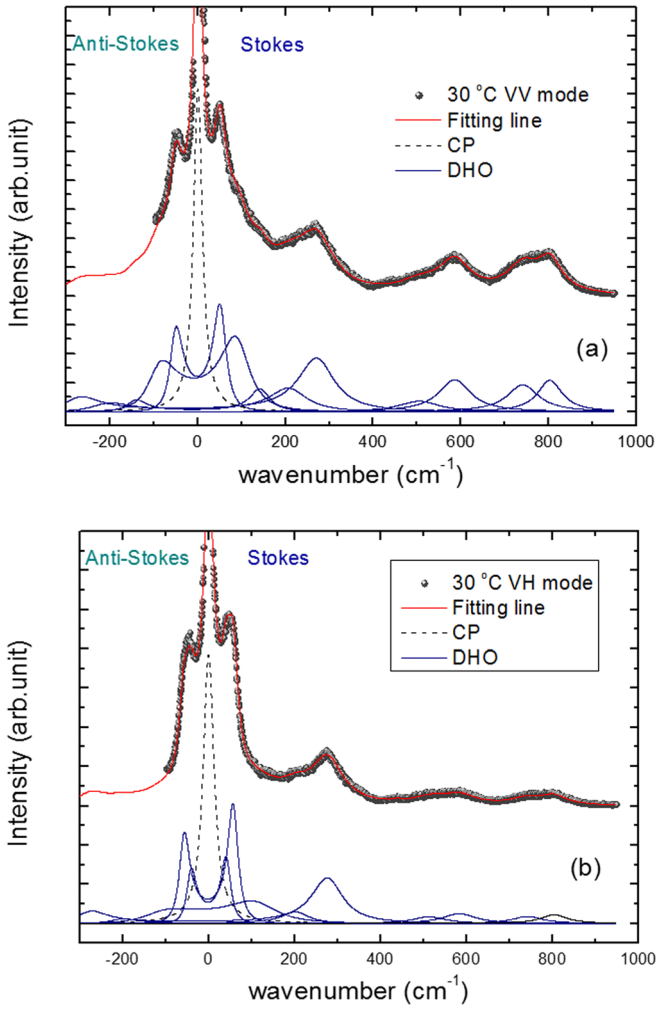

FIG. 4. Examples of multiple peak decomposition of Rama spectra measured at 30 °C in (a) VV and (b) VH geometry. The mode assignment cited results of first principles computations in $Pm\bar{3}m$.[14]

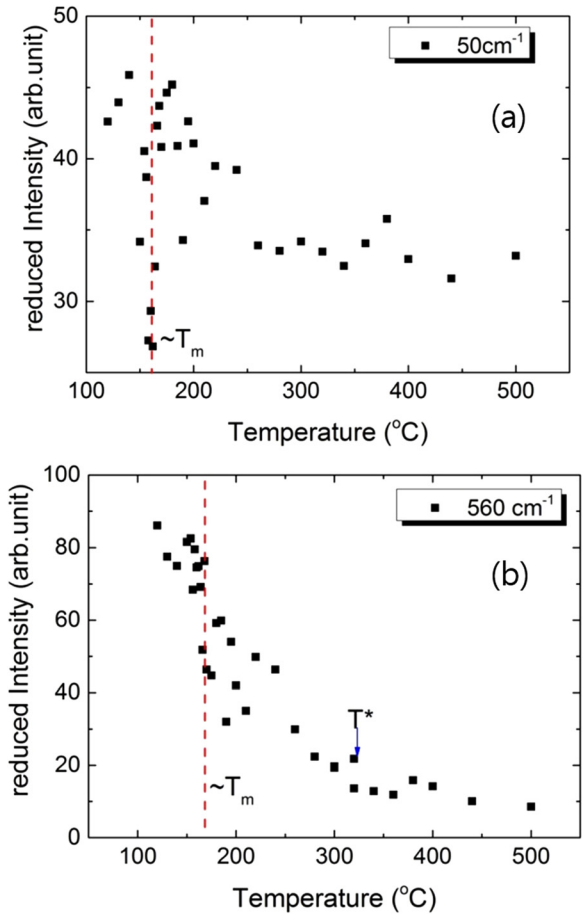

FIG. 5. Temperature dependences of the intensity of the Raman peaks located at (a) 50 cm^{-1} and (b) 560 cm^{-1} measured from unpoled PIN-PMN-PT.

spectrum shown in Fig. 4(b) also exhibits similar spectral features as those of polarized one. Usually, the characteristic length scale of COR does not show any temperature dependence. Therefore, the peak intensity of F_{2g} mode of $Fm\bar{3}m$ symmetry, which is associated with COR, does not expect to exhibit any appreciable change when the temperature passes through the Burns temperature. Fig. 5(a) shows the temperature dependence of the reduced intensity of the F_{2g} mode measured at the depolarized condition. The intensity is almost flat at high temperatures down to 250 °C. However, it shows some anomalous behavior near the dielectric maximum temperature T_m, which seems to indicate that the formation of mesoscopic polar regions near T_m has some effect on the temperature evolution of COR.

The Raman band located near 560 cm^{-1} is known to be related to PNRs, the local symmetry of which is rhombohedral.[25] The temperature dependence of the reduced intensity of this mode is shown in Fig. 5(b), which displays a noticeable increase at around 300 °C. This is the same temperature, denoted as T^*, around which the central peak grows rapidly and its half width decreases substantially as revealed by recent Brillouin scattering study.[16] This temperature was suggested to indicate the onset of rapid growth in the size of PNRs and their local phase transformation into quasi-static ones.[20,21,26] In addition, the angular dependence of the intensity variation of 560 cm^{-1} peak was compatible with the $R3m$ symmetry as predicted by Raman tensor analysis.[25]

The peak positions of an unpoled 0.26PIN-0.46PMN-0.28PT crystal do not show any appreciable changes although anomalous changes in the peak intensity could be observed as seen in Fig. 5(b). This seems to be consistent with the previous study that the dielectric constant exhibits typical frequency dispersion as observed from relaxors.[16] Recent neutron diffraction study also came to the same conclusion.[15] As a next step, the poling effect on the lattice vibration was investigated accordingly. The [001] plate was poled under the condition as described in Sec. II, and its depolarized Raman spectrum was measured upon heating. Fig. 6(a) shows temperature dependences of the Raman peak position. Some of the peaks in the low-frequency range show discontinuous changes in the mode frequency at the rhombohedral-tetragonal phase transition (T_{R-T}). Figure 6(b) shows the temperature dependence of the reduced intensity of the split peaks near 50 cm^{-1}. Both peaks exhibit step-like changes in the intensity near T_{R-T}. On the other hand, both the mode frequencies and intensities do not show any appreciable changes at the tetragonal-cubic phase transition point. According to previous dielectric study on this system,[16] the tetragonal-cubic phase transition was found to be highly diffused even under the

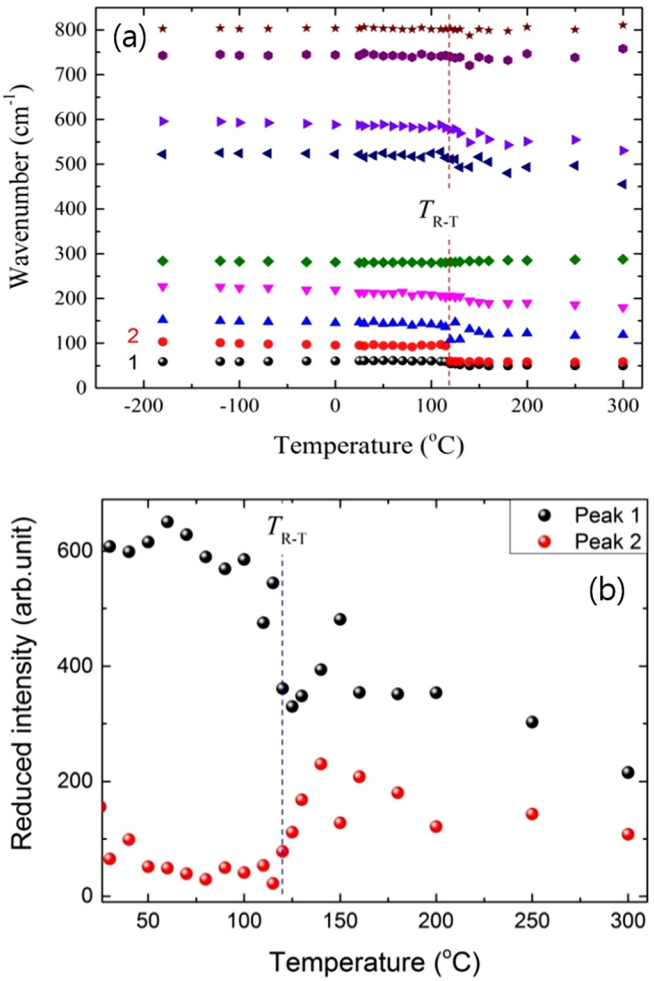

FIG. 6. Temperature dependences of (a) all the Raman peak positions and (b) the intensity of the split peaks located at ~50 cm^{-1} measured under the depolarized condition.

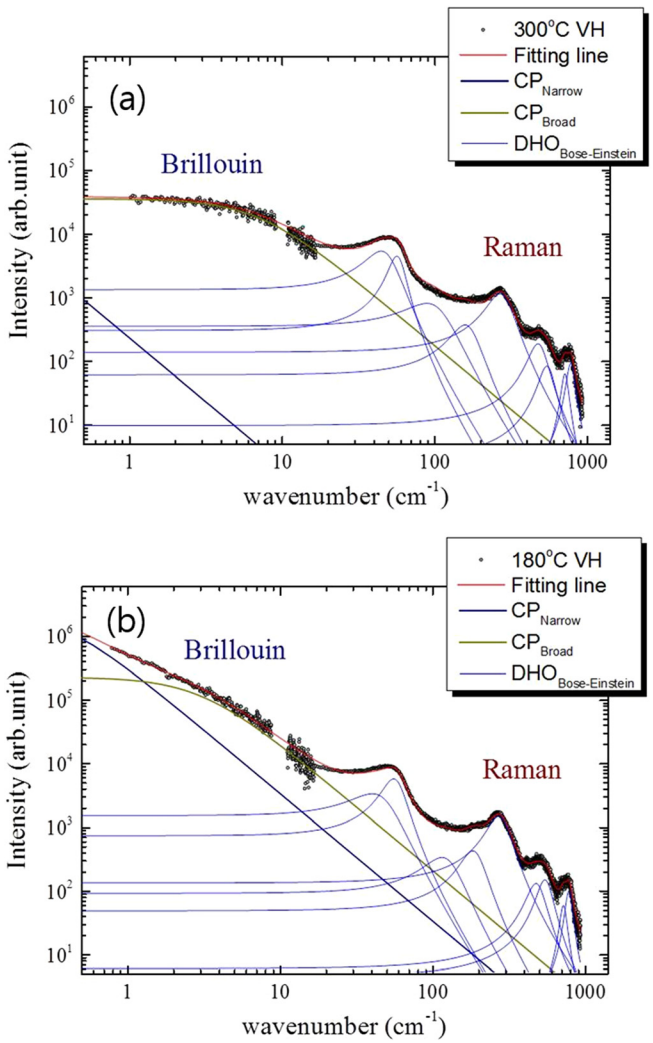

FIG. 7. Two broadband spectra of PIN-PMN-PT at the depolarized scattering geometry at (a) 300 °C and (b) 180 °C in logarithmic scales. The fitting lines consist of narrow CP, broad CP, and the response functions of the damped harmonic oscillators (DHO).

poled condition. In addition, the acoustic properties, which are sensitive to the polarization state of the sample, did not exhibit any drastic changes at T_c.[16,18] This result indicates that the apparent phase transformation reported as tetragonal-cubic phase transition does not seem to undergo a sharp, drastic change accompanied by the long-range order due to inherent disorder and strong random fields. It was suggested that the intermediate phase between T_{R-T} and T_c is characterized by the coexistence of mesoscopic polarizations and dynamic polar regions.[16] The diffuse dielectric maximum at around T_c thus indicates the characteristic temperature range where the mesoscopic polarizations disappear gradually. The effect of this diffuse phase transformation is not expected to induce any discontinuous changes in the vibrational properties, which was indeed confirmed in this study.

C. Two polarization relaxation processes

The quasi-elastic central peak was previously reported by Brillouin scattering in a limited frequency range.[16,18] The obtained relaxation time increased upon cooling indicating the slowing down behaviors of PNRs. However, the detailed spectral shape of CP could not be resolved due to the limitation of the narrow frequency window, which can only be observed by measuring the inelastic light scattering spectrum over a wide frequency range. In this context, the combination of Brillouin and Raman spectroscopy is an appropriate approach toward the exact characterization of the quasi-elastic CP of PIN-PMN-PT. For this purpose, the depolarized spectra of unpoled 0.26PIN-0.46PMN-0.28PT was measured and analyzed. Fig. 7 shows the combined spectra at two temperatures. The overlapped spectral regions around 10 cm^{-1} were used to connect the independently measured Brillouin and Raman spectra.

Each spectrum consists of broad quasi-elastic central peaks and optic phonon modes. The quasi-elastic CP was usually fitted by using a single Lorentzian model. However, the broad central-peak feature shown in Fig. 7 could not be fitted based on this model. Instead, two Lorentzian functions could be used to reproduce the spectrum similar to the case of PZN-0.07PT.[28] Fig. 7 includes the individual fitting lines of each mode and CP in addition to the best-fitted result for the whole spectrum. It is clearly seen that the two Debye relaxation processes in addition to multi-phonon lines were enough to explain the whole spectral features measured from

0.33 to 950 cm^{-1}. The appearance of CPs in relaxors has been associated with the condensation of softening transverse optical phonon resulting in the formation of PNRs at and below Burns temperature.[12,20] The fluctuations of local polarization inside the PNRs are the most probable origin of the relaxation processes observed in the CP.[31]

The quasi-elastic central peaks were fitted by using two Lorentzian functions, from which the intensity and the half-width could be derived. The obtained temperature dependences of the relaxation time (denoted as τ_{ncp}) and the CP intensity of the slower relaxation process are shown in Figs. 8(a) and 8(b), respectively. The CP intensity grows rapidly toward and shows a maximum at around T_m. τ_{ncp} is in the order of picosecond range and increases toward T_m. However, the inverse of τ_{ncp} does not exhibit a linear behavior in the paraelectric phase, as shown in Fig. 8(b). The typical critical slowing-down behavior is not observed from τ_{ncp}. One possible origin of this temperature dependence is that the local transition from dynamic to static PNRs hinders PNRs from slowing down further. To explain such a suppressed slowing down behavior which may be caused by random fields, the following empirical equation was proposed[32] in the vicinity of T_C as given by

$$\frac{1}{\tau_{ncp}} = \frac{1}{\tau_0} + \frac{(T - T_c)^{\beta}}{\Delta'}, (1 \le \beta), \quad (3)$$

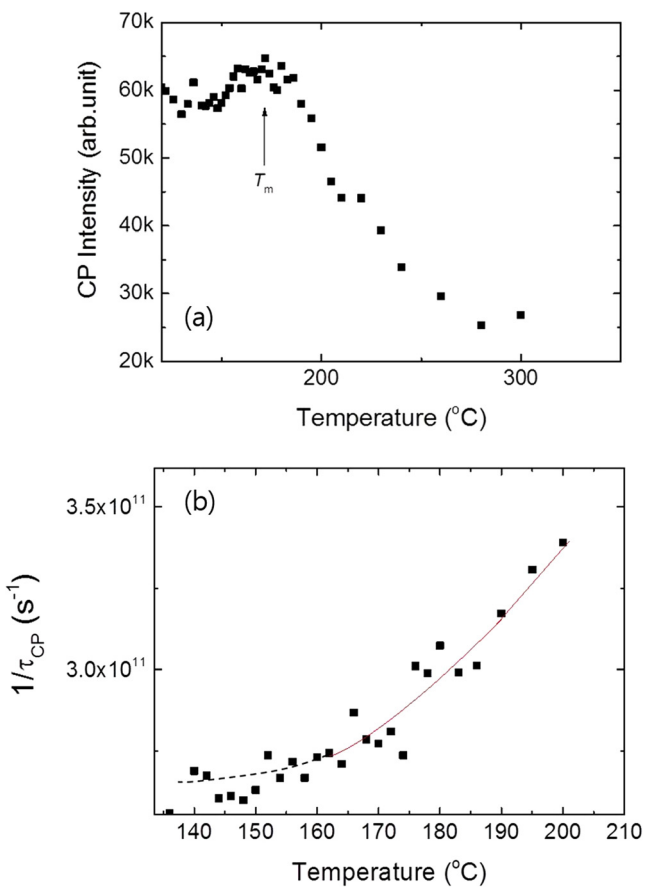

FIG. 8. Temperature dependences of (a) the intensity and (b) the inverse of the relaxation time of a narrow central peak. The solid line denotes the calculation results by Eq. (3).

where β is the stretched index, τ^0, T_C, and Δ' are fitting parameters. In the case of $\beta = 1.0$, Eq. (3) exhibits the normal critical slowing-down behavior shown from order disorder-type ferroelectrics. In the case of $\beta > 1.0$, the slowing-down behavior of the relevant relaxation process is suppressed and stretched, the degree of which may be controlled by the strength of random fields. The best-fitted result is shown as a solid line in Fig. 8(b), and the obtained value of β was 1.3. Other parameters are $\tau^0 = 3.64 \times 10^{-12}$ s, $\Delta' = 2.29 \times 10^{-9}$ K, and $T_C = 162\,^{\circ}C$.

On the other hand, the inverse of the fast relaxation time (denoted as τ_{bcp}) from the broad central peak is shown in Fig. 9 as a function of temperature. Interestingly, the inverse of τ_{bcp} shows a linear behavior near the dielectric maximum temperature, and becomes minimum at 160 °C. This kind of temperature dependence is usually observed from order-disorder type ferroelectrics that exhibit critical slowing-down behavior near the Curie point.[29,33] It is interesting that the minimum temperature of τ_{bcp} (~160 °C) shown in Fig. 9 is almost the same to 160 °C derived from τ_{ncp} by using Eq. (3). This agreement clearly indicates that a common microscopic origin, i.e., PNRs, is responsible for the two relaxation processes represented by the narrow and broad central peaks.

The origin of the two CPs and the corresponding two relaxation processes may be explained by the flipping motions of the polarization inside a PNR, as suggested by Tsukada *et al.*[28] From diffuse neutron scattering on PMN,[34] the polarization inside a PNR has been reported to align along the eight equivalent ⟨111⟩ directions in the cubic coordinates. Therefore, the slower relaxation process (the narrow Lorentzian peak) can correspond to the non-180° flipping accompanied by the change in strain, while the faster relaxation process (the broad peak) can correspond to the 180° flipping free from any change in strain.[28] However, it is not clear at the moment why the two relaxation processes occurring in PNRs exhibit different slowing-down behaviors as revealed in Figs. 8(b) and 9. Apparently, the fast relaxation process seems to associate with the "hidden" structural phase transition of unpoled 0.26PIN-0.46PMN-0.28PT, which is smeared by the strong random fields and the resulting

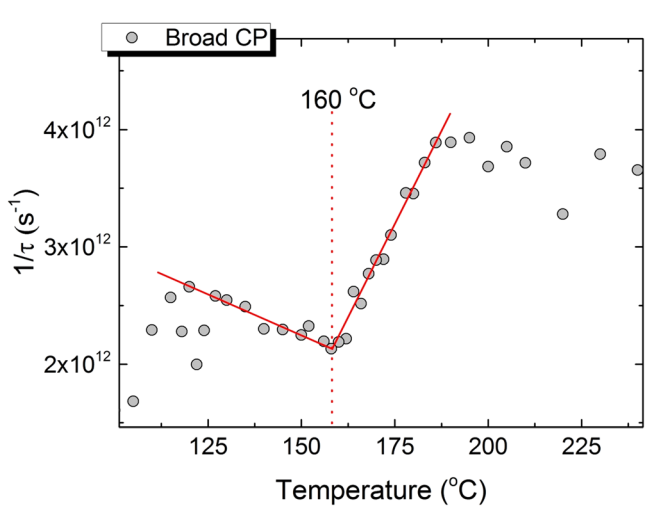

FIG. 9. The inverse of the relaxation time of the broad central peak. The solid lines denote the linear behavior of $1/\tau_{bcp}$.

diffuseness. This fact may be associated with the recent report that the field-induced phase transition occurs at almost the same temperature of ~162 °C.[15] More detailed study is necessary for getting clearer insights into the nature of these two relaxation processes.

IV. CONCLUSION

Vibrational properties and the dynamics of PNRs of a relaxor ferroelectric 0.26PIN-0.46PMN-0.28PT single crystal were studied in a broad frequency range from 0.33 to 950 cm^{-1} by Brillouin and Raman spectroscopies. The angular dependence of the intensity of a strong Raman peak located at 50 cm^{-1} was compatible with the F_{2g} mode of $Fm\bar{3}m$ symmetry, suggesting that this mode is due to the 1:1 chemical order at the B-site of this system. Broadband spectra in the paraelectric phase of unpoled 0.26PIN-0.46PMN-0.28PT exhibited two central peaks, indicating two relaxation processes associated with the polarization flipping in PNRs. The slow process showed a stretched slowing-down behavior, while the fast process exhibited a linear decrease in the relaxation time resulting in the minimum at ~160 °C. The temperature evolution of PNRs was manifested in the Raman intensity of the peak located near 560 cm^{-1}, which was known to be sensitive to PNRs. The intensity of this mode exhibited a sudden increase at ~300 °C, at which the onset of rapid growth in the size of PNRs and their local phase transformation into quasi-static ones occur. Poling the crystal along the [001] direction induced abrupt changes in some of the Raman bands at the rhombohedral–tetragonal phase transition. However, the diffuse tetragonal–cubic phase transition was not affected by the poling process, indicating that this high-temperature phase transition reported as tetragonal-cubic phase transition does not seem to be a clear structural phase transition even under the poling condition. It may be smeared out due to inherent disorder and strong random fields enhanced by the addition of PIN into PMN-PT.

ACKNOWLEDGMENTS

One of the authors (S.K.) is thankful to TRS Technologies, Inc. for providing the single crystals. This research was supported in part by the Marubun Research Promotion Foundation and the Basic Science Research Program through the National Research Foundation of Korea (NRF) funded by the Ministry of Education, Science and Technology (2013R1A1A2006582).

[1]S.-E. Park and T. R. Shrout, J. Appl. Phys. **82**, 1804 (1997).
[2]F. Li, S. Zhang, Z. Xu, X. Wei, and T. R. Shrout, Adv. Funct. Mater. **21**, 2118 (2011).
[3]Y. Hosono, Y. Yamashita, K. Hirayama, and N. Ichinose, Jpn. J. Appl. Phys., Part 1 **44**, 7037 (2005).
[4]S. Zhang, J. Luo, W. Hackenberger, and T. R. Shrout, J. Appl. Phys. **104**, 064106 (2008).
[5]X. Liu, S. Zhang, J. Luo, T. R. Shrout, and W. Gao, J. Appl. Phys. **106**, 074112 (2009).
[6]E. Sun, S. Zhang, J. Luo, T. R. Shrout, and W. Cao, Appl. Phys. Lett. **97**, 032902 (2010).
[7]F. Li, S. Zhang, Z. Xu, J. Luo, and T. R. Shrout, J. Am. Ceram. Soc. **93**, 2731 (2010).
[8]S. Zhang, G. Liu, W. Jiang, J. Luo, W. Cao, and T. R. Shrout, J. Appl. Phys. **110**, 064108 (2011).
[9]N. Yasuda, T. Fuwa, H. Ohwa, Y. Tachi, Y. Yamashita, K. Fujita, M. Iwata, H. Terauchi, and Y. Ishibashi, Jpn. J. Appl. Phys., Part 1 **50**, 09NC01 (2011).
[10]P. Finkel, K. Benjamin, and A. Amin, Appl. Phys. Lett. **98**, 192902 (2011).
[11]F. Li, S. Zhang, Z. Xu, D. Lin, J. Gao, Z. Li, and L. Wang, Appl. Phys. Lett. **100**, 192901 (2012).
[12]N. Hidayah, N. Yasuda, H. Ohwa, Y. Tachi, Y. Yamashita, and M. Iwata, Jpn. J. Appl. Phys., Part 1 **51**, 09LC06 (2012).
[13]W. D. Dong, P. Finkel, A. Amin, and C. S. Lynch, Appl. Phys. Lett. **100**, 262909 (2012).
[14]Q. Li, Y. Liu, V. Luzin, A. J. Studer, Y. Wan, Z. Li, L. Norén, R. L. Withers, and Z. Xu, J. Appl. Phys. **111**, 084110 (2012).
[15]Q. Li, Y. Liu, J. Wang, A. J. Studer, R. L. Withers, Z. Li, and Z. Xu, J. Appl. Phys. **113**, 154104 (2013).
[16]T. H. Kim, S. Kojima, and J.-H. Ko, J. Appl. Phys. **111**, 054103 (2012).
[17]G. F. Nataf, Q. Li, Y. Liu, R. L. Withers, S. L. Driver, and M. A. Carpenter, J. Appl. Phys. **113**, 124102 (2013).
[18]T. H. Kim, S. Kojima, and J.-H. Ko, Jpn. J. Appl. Phys., Part 1 **52**, 09KC01 (2013).
[19]I. G. Siny, S. G. Lushnikov, R. S. Katiya, and E. A. Rohacheva, Phys. Rev. B **56**, 7962 (1997).
[20]O. Svitelskiy, J. Toulouse, G. Yong, and Z.-G. Ye, Phys. Rev. B **68**, 104107 (2003).
[21]J. Toulouse, F. Jiang, O. Svitelskiy, W. Chen, and Z.-G. Ye, Phys. Rev. B **72**, 184106 (2005).
[22]R. Haumont, P. Gemeiner, B. Dkhil, J. M. Kiat, and A. Bulou, Phys. Rev. B **73**, 104106 (2006).
[23]A. Slodczyk, P. Daniel, and A. Kania, Phys. Rev. B **77**, 184114 (2008).
[24]Y. Yang, Y. L. Liu, S. Y. Ma, K. Zhu, L. Y. Zhang, J. Cheng, G. G. Siu, Z. K. Xu, and H. S. Luo, Appl. Phys. Lett. **95**, 051911 (2009).
[25]H. Taniguchi, M. Itoh, and D. Fu, J. Raman Spectrosc. **42**, 706 (2011).
[26]N. Waselmann, B. Mihailova, B. J. Maier, C. Paulmann, M. Gospodinov, V. Marinova, and U. Bismayer, Phys. Rev. B **83**, 214104 (2011).
[27]J.-H. Ko, D. H. Kim, and S. Kojima, Phys. Rev. B **77**, 104110 (2008).
[28]S. Tsukada and S. Kojima, Phys. Rev. B **78**, 144106 (2008).
[29]R. Ohta, J. Zushi, T. Ariizumi, and S. Kojima, Appl. Phys. Lett. **98**, 092909 (2011).
[30]N. Yasuda, H. Ohwa, J. Ohashi, K. Nomura, H. Terauchi, M. Iwata, and Y. Ishibashi, J. Phys. Soc. Jpn. **67**, 3952 (1998).
[31]K. Hirota, S. Wakimoto, and D. E. Cox, J. Phys. Soc. Jpn. **75**, 111006 (2006).
[32]S. Kojima, Jpn. J. Appl. Phys. **49**, 07HA01 (2010).
[33]J.-H. Ko, S. Kojima, T.-Y. Koo, J. H. Jung, C. J. Won, and N. J. Hur, Appl. Phys. Lett. **93**, 102905 (2008).
[34]G. Xu, G. Shirane, J. R. D. Copley, and P. M. Gehring, Phys. Rev. B **69**, 64112 (2004).